UNITED NATIONS UNIVERSITY
UNU-WIDER
World Institute for Development Economics Research

WIDER Working Paper No. 2013/071

The impact of climate change on wind and solar resources in southern Africa

Charles Fant[1] and C. Adam Schlosser[2]

July 2013

Abstract

Climate change is an issue that requires global attention and co-operation. As climate science develops an understanding of changes to the future climate state, policy makers and engineering project planners beg to know what claims can be made on the subject with a reasonable level of confidence. A common and popular mitigation strategy for reducing emissions is to build away from carbon intensive electricity production to clean energy sources like the energy produced from wind and solar irradiation. These sources themselves are climate dependent. In this study, we present a method to estimate the climate change impact on wind and solar resource potential which builds on previous studies that take a risk-based approach. The assessment combines climate projection output from the Integrated Global Systems Model, which introduces emissions and climate sensitivity uncertainty, with 19 Global Circulation Models available from the Coupled Model Intercomparison Project phase 3. Southern Africa, specifically those in the Southern African Development Community, is used as a case study. We find little agreement between Global Circulation Models and emission scenarios, resulting in a median change close to zero by 2050 in the …./

Keywords: climate change, wind energy, solar energy, southern Africa, renewable energy
JEL classification: Q42, Q47, Q54

Copyright © UNU-WIDER 2013

[1]University of Colorado Institute of Climate and Civil Systems, [2]MIT Joint Program for the Science and Policy of Global Change; corresponding author email: fantcw@colorado.edu

This study has been prepared within the UNU-WIDER project on Development under Climate Change, directed by Channing Arndt, James Thurlow, and Finn Tarp.

UNU-WIDER gratefully acknowledges the financial contributions to the research programme from the governments of Denmark, Finland, Sweden, and the United Kingdom.

ISSN 1798-7237 ISBN 978-92-9230-648-9

long-term mean of both wind speed and solar radiation (used as an indicator of change in electricity production potential). Although the extreme possibilities range from about -15 per cent to +15 per cent change, these are associated with low probability. These projected results in the long-term mean climate—and their associated probabilities—stay true to the limitations of state-of-the-art climate system models and are apt to be useful for policy and engineering planning.

The World Institute for Development Economics Research (WIDER) was established by the United Nations University (UNU) as its first research and training centre and started work in Helsinki, Finland in 1985. The Institute undertakes applied research and policy analysis on structural changes affecting the developing and transitional economies, provides a forum for the advocacy of policies leading to robust, equitable and environmentally sustainable growth, and promotes capacity strengthening and training in the field of economic and social policy-making. Work is carried out by staff researchers and visiting scholars in Helsinki and through networks of collaborating scholars and institutions around the world.

www.wider.unu.edu *publications@wider.unu.edu*

UNU World Institute for Development Economics Research (UNU-WIDER)
Katajanokanlaituri 6 B, 00160 Helsinki, Finland

Typescript prepared by Lisa Winkler at UNU-WIDER.

The views expressed in this publication are those of the author(s). Publication does not imply endorsement by the Institute or the United Nations University, nor by the programme/project sponsors, of any of the views expressed.

1 Introduction

As the threat of climate change builds, there is a push towards lower emissions. Ironically, the energy sources available without emissions are typically climate-dependent, which is especially the case for wind and solar resource. As future climates begin to behave less like past climates, modeled projections of changes in the long-term future state are attractive for national energy investment planning. Southern Africa provides an interesting case study for this analysis, specifically the Southern Africa Development Countries (SADC), which includes the Democratic Republic of Congo, Tanzania, and all countries south of these two. Energy demand in this region of the world is rising quickly, with more than 12 per cent in Mozambique and more than 10 per cent in Zimbabwe, as observed in the last couple of years, for example (SAPP 2012).

Of the countries in this region, South Africa has shown the most interest in wind and solar technology investment. There are currently three operational wind power plants in South Africa, all small-scale, although there are a few large-scale wind farms in planning. Sere Wind Farm, to be among the largest wind farms, is proposed to be built near the city of Vredendal in the Western Cape (Savannah Environmental 2007). There has also been interest in South Africa to build large-scale photovoltaics and concentrated solar power (CSP) to exploit its solar resource. Winkler (2007) found that CSP is the most affordable renewable energy option for decreasing emissions in South Africa. Although there are no existing large-scale CSP plants in southern Africa, the South African electricity utility, Eskom, has recently invested in planning a 100 MW CSP plant in the Northern Cape near the city of Upington (Eskom 2012), and the South African government is promoting a 5,000 MW solar park in the Northern Cape (Zawilska et al. 2012).

The implications of possible changes in usable wind and solar potential must be well understood for future planning purposes. Some reports have noted that wind speed and cloudiness are likely to change in the future. Wind speed and cloudiness are strongly influenced by temperature differentials. Since climate change is generally characterized by changes in global temperature, one can easily make a connection between increasing emissions and these climate parameters, concluding that changes in temperature can directly affect surface wind speed and solar irradiation. These climate parameters are also influenced by physical phenomena like El Nino Southern Oscillation (ENSO) and Madden-Julian Oscillation (MJO), which could behave differently in the future (Rauthe et al. 2004). Meehl et al. (2007) report that peak wind speeds will likely increase with increasing temperatures, and Hazeleger (2005) suggests that the trade winds in particular are likely to change. Land surface changes can affect local cloudiness and could be amplified in urban areas (Denman et al. 2007), but making connections between climate change and changes in solar irradiation is a complicated matter (Hegerl et al. 2007). In fact, understanding the impacts of climate change on both aerosols in the atmosphere and boundary layer wind speed are problematic because of the spatial scale of current Global Circulation Models (GCMs). Studies have been done on understanding the impact of climate change on wind and solar parameters, but the subject is less studied than the impacts on biophysical sectors, e.g. agriculture.

1.1 Wind speed and solar irradiation in a Global Circulation Model

First, the usefulness of climate projections from GCMs should be addressed. The general concern being what the GCM output can tell us about the future of renewable resource availability given the inherent uncertainties of climate modeling techniques currently in practice. The full spectrum of this concern is outside the scope of this study, and therefore will not be answered in great detail. Instead, we will attempt to use the general consensus on GCM uncertainty to stay within the area where GCM output data are considered useful.

In order to understand the usefulness of GCM output, we must understand how wind and solar variables are understood in a GCM. Because wind is the movement of air in the atmosphere, important for tracking convective transfers of temperature and moisture, it is an essential process in the global climate system. Solar forcing is also essential, since it is the source of the majority of the energy. For these reasons, wind and solar resources are very common topics in climate science and much emphasis is placed on modeling these as accurately as possible. In a GCM, wind speed is modeled as an average over a large cube in space. The GCMs provide wind speed output at 10 m, an estimation derived from the wind speed values of the atmospheric layer closest to the surface. Vertical layers in a GCM are typically defined by constant pressure, meaning that the layer heights change in space and time. These pressure layers are also unevenly distributed so that a finer resolution is achieved near the surface. In a typical GCM, the atmosphere is modeled with about 10–20 layers reaching to about 30 km. GCMs also represent the climate at a coarse horizontal resolution of about 250 to 600 km (IPCC 2012). The problem with dividing the atmosphere into large cubes is that many processes occur at a much smaller scale. These large cubes are not ideal for modeling changes in small-scale wind, which is highly dependent on the effects of elevation, surface roughness, and convection. Clouds and other aerosols can also change at smaller scales than a typical GCM grid. Cloud feedbacks in particular are considered the highest uncertainty in current GCM practice (Randall et al. 2007). Cloud cover fraction output is usually estimated based on relative humidity values in each GCM cube. These estimations of small-scale processes on a larger scale are called 'parameterization.' There are many parameterization schemes for estimating changes in wind speed and aerosols in the various layers of the atmosphere, and the Coupled Model Intercomparison Project Phase 3 (CMIP-3) GCMs employ a variety of these schemes.

1.2 Previous attempts to characterize the future wind and solar state

In the past, climate change impact studies have typically involved one of two approaches: (i) a climate sensitivity analysis using a wide, unguided range of future climate possibilities (e.g. Kurukulasuriya 2006, Wilks 1992); or (ii) use of select climate model output, typically GCMs from the Coupled Model Intercomparison Project (CMIP), commonly referred to as the Intergovernmental Panel for Climate Change (IPCC) Fourth Assessment Report (AR4) models (e.g. Liu et. al 2013; Arndt et. al 2010; World Bank 2009; Immerzeel 2008). The output of these models is applied directly in a climate change impact-modeling framework to assess the impacts of climate change, resulting in a limited set of future scenarios. Research on the climate change impact on wind and solar resources follows a similar pattern, although recently there has been more activity in (ii) than (i). These studies are discussed below.

Pryor et al. (2006) attempted to estimate changes in the mean and upper percentile of wind speed in northern Europe. The authors used daily output from ten GCMs for the A2 scenario, fitting a regression model that predicts Weibull distribution parameters fitted from station data. The model was fit using mean and standard deviation of 500 hectopascals relative vorticity and mean of daily sea level reduced pressure gradients from the historical GCM runs. Then, using future outputs of the predictors, they were able to produce estimations for ten possible futures of both the wind speed and wind power state, predicting the mean and 90^{th} percentile of each. They found that there was not much agreement between the GCMs, and no confident conclusion could be made about changes in wind characteristics by 2050 for the wind stations used. Looking further in the future, their study suggests that mean and 90^{th} percentile wind speeds will decrease slightly by 2100. Sailor et al. (2008) studied possible changes to wind speed and wind power produced over the northwestern USA. They used two GCMs and two Special Reports on Emissions Scenarios (SRES). They found that the historical results from the GCMs did not match weather station measurements in the area. Applying a statistical downscaling technique to the raw GCM output, they found, of course, that the agreement improved. They compared the two SRESs from each GCM and found that there was not much agreement, even though the same model was used. The study suggests that summertime winds will decrease by 5–10 per cent in the area, and winter winds will either slightly increase or stay the same. Using typical hub heights and a common turbine power curve, they found that the power produced in the summer could decrease by about 40 per cent. Pryor et al. (2012) used a suite of 13 simulations from a combination of four Regional Climate Models (RCMs) nested in reanalysis data and four global climate models. These simulations were compared to independent observations and the North American Regional Reanalysis (NARR) over the contiguous USA. The RCMs were found to exhibit some skill in reproducing historical wind patterns, although the RCM architecture seems to be the primary cause of variance between models rather than the lateral boundary conditions. The study goes on to estimate changes in various wind statistics averaged over 2041–60, finding some agreement between models in terms of sign. The simulations suggest that intense wind speeds are likely to decrease, especially in the western USA by 2050. Seljom et al. (2011) links ten GCM-scenario pairs to an RCM to estimate climate change effects on the Norwegian energy sector. Changes in wind, solar irradiation, and heating and cooling demand, among others, were estimated by interpolating the RCM results to 20 geographic locations: seven for solar, and 13 for wind. The study found that while solar radiation and hydropower changes were significant in some of the GCM-scenario projections, changes in wind were minor, with the maximum change for all locations and months around 4.8 per cent by 2050. Fenger et al. (2007) came to a similar conclusion of changes in wind over Norway. Pan et al. (2004) used a RCM to estimate seasonal changes in solar radiation simply by raising greenhouse gas concentrations in the regional model. A decreasing trend was found in the seasonal mean of global solar radiation of about 0–20 per cent over the entire USA. This trend was most noticeable in the western USA during fall, winter, and spring.

We have three main observations from the literature. First, there have been few studies that have looked at future changes in solar resource, likely due to the uncertainties in GCM cloud cover estimations discussed previously. Second, the studies that have estimated changes in wind speed have only found small long-term mean changes, the largest at 5–10 per cent; although, Sailor et al. (2008) claim that small reductions in wind speed could result in large reductions in power produced. And third, these studies did not find much agreement between historical observations and GCM output, between the different GCMs, or the SRES scenario outputs of a single GCM.

In general, research on the impacts of climate change has followed a similar pattern. The past climate state is studied briefly, and then information from climate models is applied. Next, climate change impact studies carefully apply a limited number of these scenarios in an intelligent way to understand the future climate state. Since climate models are very computationally expensive, only a limited amount of scenarios can be effectively run to produce useful output, resulting in a scarcity of possible future scenarios. Schlosser et al. (2011) present a method to expand the full set of CMIP-3 GCMs to a large pool of climate predictions. The Integrated Global Systems Model (IGSM) (Sokolov et al. 2009 and Webster et al. 2011) developed near-surface temperature and precipitation projections at the zonal spatial scale for 400 scenarios representing economic and climate uncertainty. A Taylor expansion technique, described by Schlosser et al. (2011), was used to expand from the zonal level of detail in the longitudinal direction. This transformation requires the construction of climate change pattern kernels, which vary through time as global temperature changes. The full ensemble of climate change projections is produced through the numerical hybridization of the IGSM zonal trends, with pattern kernels of regional climate change from 17 of the CMIP-3 models. This ensemble of future climate projections is called 'hybrid frequency distributions' (HFDs). Using this framework, 6,800 climate projections are produced for each of the five CO_2 emissions policy scenarios. The HFDs, however, currently provide changes in precipitation and temperature, which are useful for biophysical impact modeling, but do not yet provide changes in other climate parameters. Also, the establishment of these HFD projections requires a selection among the SRES scenarios—namely, A2, A1b, and B1—because emission-forcing scenarios are already represented in the five policy scenarios. Fortunately, Schlosser et al. (2011) found strong correlations between the scenarios for precipitation and temperature, suggesting that the differences between model outputs are driven almost entirely by model choice, while SRES choice is insignificant.

2 Data and method

First, a baseline needs to be established with which to compare the projected changes in climate. With the advancement of satellite utility and measurements, global datasets are becoming more popular for areas with a limited or unreliable set of historical data. For this study, the MERRA (Modern-Era Retrospective for Research and Analysis) reanalysis dataset will be used to represent the base climate for all solar and wind characteristics (Rienecker et al. 2011). The MERRA dataset is attractive because it attempts to represent a balance between satellite, station, and modeled climate gridded globally at an hourly time-step from 1979 to 2009. MERRA improves on the representation of the hydrologic cycle and uses a large repository of conventional observations from various sources, as well as satellite radiance data. Source: authors' creation.

Figure 1 shows the mean wind speed over southern Africa, calculated using the log wind profile as described in Gunturu and Schlosser (2012). As shown, most of the onshore wind resource is in the southern and northeastern parts of the SADC region, with clusters of moderate wind speed in between. There is a large area of low wind speeds in the northwestern part of the map, comprised of the countries in the Congo River Basin and almost all of Angola. Source: authors' creation.

Figure 2 shows the mean incident solar radiation at the surface. Most of the solar resource is in the southwest, surrounding Namibia and extending out to Zimbabwe, and in the northeast in Tanzania and Kenya.

The seasonal mean wind speed and solar radiation at select grids are shown in Table 1. The grid selected for wind speed is meant to represent the proposed Sere wind farm, previously discussed. Similarly, the solar radiation values were calculated from the grid containing the site of the proposed large CSP plant. As shown, the December-January-February (DJF) season has the potential for the most power produced, while the June-July-August (JJA) season has the least potential for both sources; although, the March-April-May (MAM) season has equally low potential for wind.

Now, to understand changes in the future state of these resources, we explore the usefulness of a risk-based approach. Previous studies have used varying techniques to better understand the future state of wind and solar resource, using between one and 13 future scenarios. Given the recent advances in climate science provided through the HFD method, a larger pool of future scenarios can likely be generated, providing a more complete picture of the *risk* associated with climate change. Basically, a connection needs to be made between the methods presented in Schlosser et al. (2011) and changes in both wind and solar resource.

The first attempt to make these connections was to use the outputs provided by the HFD data—monthly changes in temperature and precipitation—and to relate these with wind speed changes. First, we needed to find a meaningful relationship between the predictors and the predictand in the historical data. We used the MERRA data for this investigation—monthly precipitation and temperature aggregated to the provincial level. Besides using the temperature and precipitation data directly, we decided to use differences between onshore and offshore temperature. The final predictors were monthly temperature at the surface, precipitation, and onshore/offshore temperature gradients.

Since the intermittency of wind and solar resource is important to energy grid planning that might not be captured with mean only, we decided to count hours in each month within certain ranges of WPD, resulting in three power-potential measurements within a month. We also included mean and median WPD. In the end, we have five predictands: mean wind speed, hours of no power, hours of low power, and hours of high power. At first, we found that there was a fairly significant relationship between all of these predictands and at least one of the four predictors. Then, concerned that we might be finding a false relationship, we removed the seasonal mean from the predictors. After removing this mean, the predictors and predictands seem to have no significant relationship. This method was abandoned.

After finding that there is no significant relationship with the typical HFD output, we tried a new approach. A majority of the GCMs report both wind speed predictions at 10 m and incident solar radiation at the surface. Using these outputs, we have related global temperature rises with the gridded wind speed and solar radiation changes for each of the GCM-SRES pairs where data are available from the CMIP-3 database. The seasonal mean was removed from each variable based on the mean of the first ten years. These differences from the mean are what we use for the model.

We first checked for a relationship by calculating a Spearman rank correlation coefficient between these two variables for four three-month periods. Figure 3 shows an example of a global map displaying these correlation coefficients. We find that in the most extreme cases, the correlation is about 0.5 or -0.5. These values are fairly significant given that the predictor is a global parameter, and given that the findings from the previous studies, mentioned in the literature review, find only small, if any, changes to wind speed by 2050. A qualitative observation from these maps is that the correlation values appear to be showing a coherent global pattern, implying that the correlation is at least partly driven by a natural relationship.

We then look at two locations in South Africa with characteristically different wind speed patterns. The first is near the border of the Western Cape and Northern Cape. The second location is located in the northern part of the Limpopo province. First, although the highest correlation values are close to +/-0.5, the correlations are fairly low for these two locations for the majority of the GCM-SRES pairs. The other concern is that there is not a strong agreement between the SRESs for a given model, an important finding that drove the former HFD framework smoothly. If there was a strong agreement, we could assume that variance across model output is driven by differences in model structure. Instead, we find that the variance across model output must also be driven by the internal variability of the chaotic climate system that is modeled. This kind of uncertainty is difficult to quantify and has been left for future research.

We then move on to estimating changes in wind and solar resource potential. A locally weighted polynomial regression, as explained in Rajagopalan and Lall (1998), is used as the statistical model to represent the relationship of global mean temperature to changes in both wind speed and incident solar radiation, although other statistical models could be used. We then estimate the changes in wind speed and solar radiation based on global temperature changes produced from the 400 IGSM scenarios. Each of the CMIP-3 GCMs with wind speed output data are uniquely represented, which results in a maximum of 7,600 scenarios if the A1b scenario outputs are used. We use the CMIP-3 output data as an example because they are already well established, but the method could be applied to the CMIP-5 data. Also, since the model is set up to project changes from a modeled history, we bypass the issue of not matching the historical climate commonly found in previous studies.

3 Results

3.1 Results at selected sites

Due to the uncertainties of GCM output previously discussed, we restrict these results to projections in long-term mean seasonal changes in resource potential. Wind speed changes and changes in solar radiation are predicted to 2050 for southern Africa by averaging results over 11 years, from 2045 to 2055. As an example, wind speed changes for the selected wind site are shown in Figure 4. Here, we present results for the Unconstrained Emissions (UE) and Level 2 Stabilization (L2S). IGSM policy cases coupled with the models derived from each SRES scenario output. As shown, the changes are relatively small, with modes close to zero and extremes from -1.5 to +1.5 m/s. In most seasons, the results tend to suggest an increase in wind

speed, which would increase wind power potential; although, during the JJA season, there is a slight tendency toward wind speed decreases, especially in the extremes. This result is undesirable because JJA is the season with the lowest wind speeds according to the base data, and the season of highest energy demand in South Africa. Still, the results suggest that wind speed changes would be insignificant by 2050 at the selected wind site for all seasons, with a small chance of either a positive or negative change of about 20 per cent.

Figure 5 shows the changes in solar radiation for the selected solar site. The mode for all four seasons is slightly negative in almost all scenarios, but the solar radiation changes for the selected site are likely small, if not zero. In the extreme results, changes range from about -20 to + 20 W/m^2, which equates to approximately 10 per cent of the mean.

Notice that the results depend somewhat on the SRES scenario. This was not the case for the method used to produce precipitation and temperature change ensembles in Schlosser et al. (2011). In fact, in most cases, the differences between the results from the SRES scenario are about the same magnitude as the differences in IGSM policy cases, i.e. UE or L2S. The UE results tend to have a wider and shorter distribution than the L2S case, implying more likely extreme changes, but no obvious pattern was observed in the differences from the SRES scenario choice. Given that all of the models produce results for the A1b scenario—19 models total—and only some produce results for the other two scenarios, the A1b model is selected for the remaining results. Also, of the three scenarios, A1b presents a medium emissions forcing case, while A2 and B1 represent the extremes.

3.2 Results over southern Africa

In the following maps, we shift focus to the JJA season because this is the season of high heat demand in South Africa. Figure 6 shows the geographic variation of changes in wind speed for the JJA season over southern Africa modeled from the A1b output. The 20^{th}, 50^{th}, and 80^{th} percentiles are shown to represent the distribution of results over the 7,600 scenarios. The top row presents the L2S policy case, and the bottom row, the UE policy case. For the most part, wind speed changes are small in southern Africa. The most extreme wind speed changes occur in the ocean, where the median change ranges from about -0.5 m/s off the southern coast of South Africa to +0.4 m/s off the coast of Namibia to the west, and around the boarder of Mozambique and South Africa to the east. These same patterns emerge through all six maps. Inland, there is a cluster of increases in wind speed along the border of South Africa and Botswana that is especially prevalent in the UE 80^{th} percentile. Further northwest, along the coast of the Democratic Republic of the Congo at the mouth of the Congo River and surrounding, is another area of projected increased wind speed. In general, although the differences in the results from the two policy cases are relatively small, the same pattern emerges—UE presents a wider range of possible wind speed changes, as shown in the 20^{th} and 80^{th} percentiles.

Figure 7 shows the geographic variation of changes in solar radiation for the JJA season. This figure uses the same layout as Figure 6. Changes in solar radiation are small, even in the extremes. The median shows a decrease in solar radiation over most of the region, except an area around Malawi, west along the equator, and the southwestern tip of South Africa. The area with the strongest decrease extends from Kenya in the east and through Angola and Namibia in the

west. These tendencies persist through the distribution, emerging in the 20th and 80th percentile maps. Also, we again see the extremes stronger in the UE policy case than the L2S policy case. Although different geographic patterns emerge depending on the season modeled, changes in wind speed and solar radiation are relatively small for all seasons and regions of southern Africa. In looking at the annual mean change, some patterns do emerge. For wind, mean wind speeds are increasing offshore west of South Africa and Namibia and east of South Africa and Mozambique, but decreasing south of South Africa. These patterns persist in the extremes reaching a minimum of about -1.5 m/s, to a maximum of +1.5 m/s in the UE case, while the range for the L2S case reaches extremes of -1 m/s to +1 m/s. Onshore are smaller changes, with increasing wind clustering along the border of Botswana and South Africa extending to southern and central Mozambique. Decreases in wind speed extend to a larger region—strongest in Kenya and Tanzania, but extending out to Angola, Namibia and western South Africa. The onshore changes range from about -1 m/s to +1m/s in the UE case, and -0.4 m/s to +0.5 m/s in the L2S case. For annual mean changes in solar radiation, we see increases along most of the onshore area except near the coast. The areas of largest decrease in solar radiation are found along the western coast, especially near the border of Namibia and South Africa, and another area clustering around the Tanzania-Kenya-Uganda boarders. The extremes range from about -35 W/m^2 to +35 W/m^2 in the UE case, and about -18 W/m^2 to +12 W/m^2 in the L2S case.

4 Closing remarks

As a response to previous studies that have tried to dissect GCM output from a select set of model results in order to understand the future state of wind and solar resource potential, we have shown a method that introduces emissions, climate sensitivity, and regional climate uncertainty. A statistical model was used to expand the HFD approach to include wind and solar parameter estimations, effectively producing a portfolio of possible outcomes. The results, even in the extremes, are consistent with previous studies, which found only small changes to wind and solar potential by 2050. We also found that the GCMs report a wide range of results. These differences in output exist across the models as well as across the emission scenarios, resulting in a central tendency close to zero change when combined. Since the emission uncertainty in the presented results exists in the different models produced from the three SRES scenario outputs as well as the IGSM scenarios, and a commonality was not found among the SRES scenario output as was found in Schosser et al. (2011), further research is required. Regardless, this study has found that either the long-term mean wind and solar resource potential will likely remain unchanged by 2050, or that the uncertainty of the GCM models is much too large, even with state-of-the-art climate science, to make claims on the future state of these resources.

References

Arndt C., K. Strzepek, F. Tarp, J. Thurlow, C. Fant, and L. Wright (2010). 'Adapting to Climate Change: an Integrated Biophysical and Economic Assessment for Mozambique'. *Sustain Sci*, 6(1): 7–20.

Denman, K.L., G. Brasseur, A. Chidthaisong, P. Ciais, P.M. Cox, R.E. Dickinson, D. Hauglustaine, C. Heinze, E. Holland, D. Jacob, U. Lohmann, S. Ramachandran, P.L. da Silva Dias, S.C. Wofsy, and X. Zhang, (2007). 'Couplings between Changes in the Climate

System and Biogeochemistry', in S. Solomon, D. Qin, M. Manning, Z. Chen, M. Marquis, K.B. Averyt, M. Tignor, and H.L. Miller (eds), *Climate Change 2007: The Physical Science Basis. Contribution of Working Group I to the Fourth Assessment Report of the Intergovernmental Panel on Climate Change*. Cambridge and New York: Cambridge University Press.

Eskom (2012). Available at: www.eskom.co.za (accessed October 2012).

Fenger, J. (2007). 'Impacts of Climate Change on Renewable Energy Sources: Their Role in the Nordic Energy System: A Comprehensive Report Resulting from a Nordic Energy Research Project'. Copemhagen: Nordisk Ministerrad.

Gunturu, U. B., and C.A. Schlosser (2011). 'Characterization of Wind Power Resource in the United States and its Intermittency.' *MIT Joint Program on the Science and Policy of Global Change*, Cambridge, 24(14): 3624–3648.

Hazeleger, W. (2005). 'Can Global Warming Affect Tropical Ocean Heat Transport?' *Geophys. Res. Lett.*, 32, L22701, doi:10.1029/2005GL023450.

Hegerl, G.C., F.W. Zwiers, P. Braconnot, N.P. Gillett, Y. Luo, J.A. Marengo Orsini, N. Nicholls, J.E. Penner, and P.A. Stott, (2007). 'Understanding and Attributing Climate Change', in S. Solomon, D. Qin, M. Manning, Z. Chen, M. Marquis, K.B. Averyt, M. Tignor and H.L. Miller (eds), *Climate Change 2007: The Physical Science Basis. Contribution of Working Group I to the Fourth Assessment Report of the Intergovernmental Panel on Climate Change* Cambridge and New York: Cambridge University Press.

Immerzeel, W (2008). 'Historical Trends and Future Predictions of Climate Variability in the Brahmaputra Basin'. *International Journal of Climatology*, 28(2): 243–254.

Intergovernmental Panel on Climate Change (IPCC). (2012). Data Distribution Centre Available at: http://www.ipcc-data.org (accessed September 2012).

Kurukulasuriya P., R. Mendelsohn, R. Hassan, J. Benhin, T. Deressa, M. Diop, H.M. Eid, K.Y. Fosu, G. Gbetibouo, S. Jain, A. Mahamadou, R. Mano, J. Kabubo-Mariara, S. El-Marsafawy, E. Molua, S. Ouda, M. Ouedraogo, I. Sene, D. Maddison, S.N. Seo, A. Dinar (2006). 'Will African Agriculture Survive Climate Change?' *The World Bank Economic Review*, 20(3): 367–388.

Liu J.J., C.C. Folberth, H.H. Yang, J.J. Röckström, K.K. Abbaspour, A.J. Zehnder (2013). 'A Global and Spatially Explicit Assessment of Climate Change Impacts on Crop Production and Consumptive Water Use'. *PLoS One*, 8(2): e57750–e57750.

Meehl, G.A., T.F. Stocker, W.D. Collins, P. Friedlingstein, A.T. Gaye, J.M. Gregory, A. Kitoh, R. Knutti, J.M. Murphy, A. Noda, S.C.B. Raper, I.G. Watterson, A.J. Weaver and Z.-C. Zhao (2007). 'Global Climate Projections', in S. Solomon, D. Qin, M. Manning, Z. Chen, M. Marquis, K.B. Averyt, M. Tignor, and H.L. Miller (eds), *Climate Change 2007: The Physical Science Basis. Contribution of Working Group I to the Fourth Assessment Report of the Intergovernmental Panel on Climate Change* Cambridge and New York: Cambridge University Press.

Pan, Z., M. Segal, R.W. Arritt, and E.S. Takle (2004). 'On the Potential Change in Solar Radiation over the US due to Increases of Atmospheric Greenhouse Gases.' *Renewable Energy*, 29(11): 1923–1928.

Pryor, S.C., J.T. Schoof, and R.J. Barthelmie (2006). 'Winds of Change?: Projections of Near-surface Winds under Climate Change Scenarios'. *Geophys. Res. Lett.*, 33, L11702, doi:10.1029/2006GL026000.

Pryor, S.C., R.J. Barthelmie, and J.T. Schoof (2012). 'Past and Future Wind Climates over the Contiguous USA based on the North American Regional Climate Change Assessment Program Model Suite'. *Journal of Geophys. Res.*, 117, D19119, doi:10.1029/2012JD017449.

Rajagopalan, B., and U. Lall (1998). 'Locally Weighted Polynomial Estimation of Spatial Precipitation'. *Journal of Geographic Information and Decision Analysis*.

Randall, D.A., R.A. Wood, S. Bony, R. Colman, T. Fichefet, J. Fyfe, V. Kattsov, A. Pitman, J. Shukla, J. Srinivasan, R.J. Stouffer, A. Sumi, and K.E. Taylor (2007). 'Climate Models and Their Evaluation', in S. Solomon, D. Qin, M. Manning, Z. Chen, M. Marquis, K.B. Averyt, M. Tignor, and H.L. Miller (eds), *Climate Change 2007: The Physical Science Basis. Contribution of Working Group I to the Fourth Assessment Report of the Intergovernmental Panel on Climate Change* Cambridge and New York: Cambridge University Press.

Rauthe, M., A. Hense, and H. Paeth (2004). 'A Model Intercomparison Study of Climate Change Signals in Extratropical Circulation'. *International Journal of Climatology*, 24 (5): 643–662.

Rienecker, M.M., M.J. Suarez, R. Gelaro, R. Todling, J. Bacmeister, E. Liu, , M.G. Bosilovich, , S.D. Schubert, L. Takacs, G.-K. Kim, S. Bloom, J. Chen, D. Collins, A. Conaty, A. da Silva, W. Gu, J. Joiner, R.D. Koster, R. Lucchesi, A. Molod, T. Owens, S. Pawson, P. Pegion, , C.R. Redder, R. Reichle, F.R. Robertson, A.G. Ruddick, M. Sienkiewicz, and J. Woollen (2011). 'MERRA: NASA's Modern-Era Retrospective Analysis for Research and Applications.' *Journal of Climate*, 24(14): 3624–3648.

Sailor, D. J., M. Smith, and M. Hart (2008). 'Climate Change Implications for Wind Power Resources in the Northwest United States'. *Renewable Energy* 33, 2393–2406.

Southern Africa Power Pool (SAPP) (2012). 'Annual Report 2012'. Available at: www.sapp.co.zw/docs/SAPP%202012%20annual%20report.pdf

Savannah Environmental (2007). 'Final Scoping Report: Proposed Wind Energy Facility and Associated Infrastructure, Western Cape Province'. Report prepared for Eskom Holdings Limited.

Schlosser, C.A., X. Gao, K. Strzepek, A. Sokolov, C.E. Forest, S. Awadalla, and W. Farmer (2011). 'Quantifying the Likelihood of Regional Climate Change: A Hybridized Approach'. *MIT Joint Program on the Science and Policy of Global Change*, 26: 3394–3414, doi: http://dx.doi.org/10.1175/JCLI-D-11-00730.1

Seljom, P., E. Rosenberg, A. Fidje, J.E. Haugen, M. Meir, J. Rekstad, and T. Jarlset (2011). 'Modelling the Effects of Climate Change on the Energy System—A Case Study of Norway'. *Energy Policy*, 38(11): 7310–7321.

Sokolov, A.P., P.H. Stone, C.E. Forest, R. Prinn, M.C. Sarofim, M. Webster, S. Paltsev, C.A. Schlosser, D. Kicklighter, S. Dutkiewicz, J. Reilly, C. Wang, B. Felzer, J.M. Melillo, and H.D. Jacoby (2009). 'Probabilistic Forecast for Twenty-First-Century Climate Based on Uncertainties in Emissions (Without Policy) and Climate Parameters'. *Journal of Climate*, 22: 5175–5204.

Webster, M., A. P. Sokolov, J. M. Reilly, C.E. Forest, S. Paltsev, C.A. Schlosser, C. Wang, D. Kicklighter, M. Sarofim, J. Melillo, R.G. Prinn, and H.D. Jacoby (2011). 'Analysis of Climate Policy Targets under Uncertainty'. *Climatic Change*, 112(3–4): 569–583.

Wilks, D.S. (1992). 'Adapting Stochastic Weather Generation Algorithms for Climate Change Studies'. *Climatic Change*, 22 (1): 67–84

Winkler, H. (ed) (2007). 'Long Term Mitigation Scenarios: Technical Report'. Prepared by the Energy Research Centre for Department of Environment Affairs and Tourism, Pretoria, October 2007. Available at: www.erc.uct.ac.za/Research/publications/07-Winkler-LTMS-Technical%20Report.pdf

World Bank (2009). 'The Cost to Developing Countries of Adapting to Climate Change: New Methods and Estimates. The Global Report of the Economics of Adaption to Climate Change Study'. Washington, DC: World Bank. Available at: http://siteresources.worldbank.org/EXTCC/Resources/EACC-june2010.pdf

Zawilska, E., M.J. Brooks, A.J. Meyer (2012). 'A Review of Solar Resource Assessment Initiatives in South Africa: The Case for a National Network'. Boulder, CO: American Solar Energy Society.

Table 1: Mean seasonal wind speed and incident solar radiation for selected wind and solar sites.

	Wind Speed (m/s)	Solar Radiation (W/m^2)
DJF	5.5	359
MAM	4.2	233
JJA	4.2	184
SON	5.1	315

Source: authors' creation.

Figure 1: Geographic variation of mean wind speed (m/s) at 50m over southern Africa

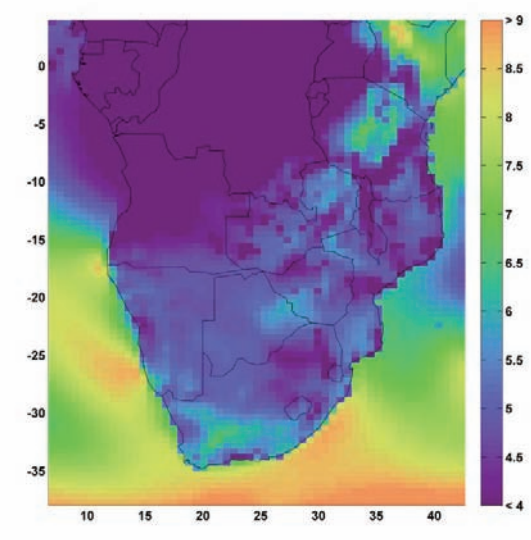

Source: authors' creation.

Figure 2: Geographic variation of mean incident solar radiation (W/m^2) over southern Africa

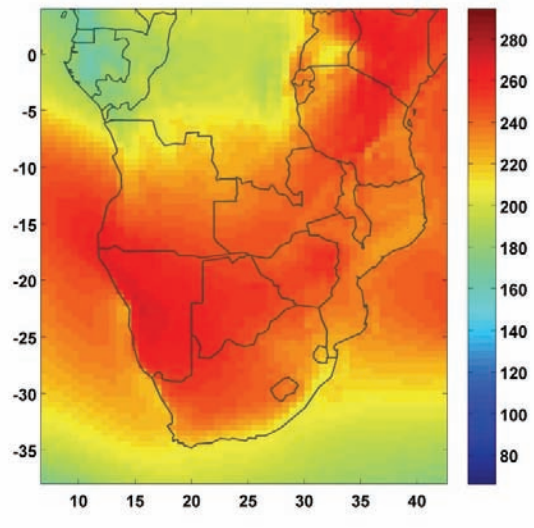

Source: authors' creation.

Figure 3: Correlation of wind speed cubed and global temperature rise for the CSIRO MK3.5 model running the A1b scenario for the four seasons

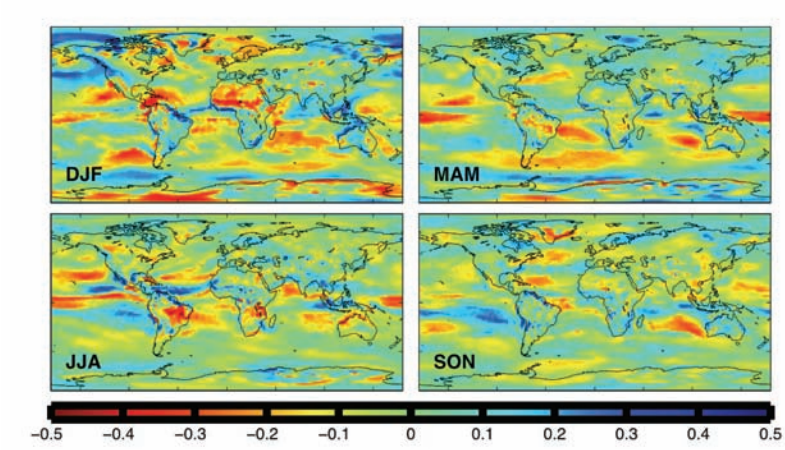

Source: authors' creation.

Note: In the top left is the correlation with the Dec/Jan/Feb (DJF) season; in the top right is the Mar/Apr/May (MAM) season; in the bottom left is the Jun/Jul/Aug (JJA) season; and in the bottom right is the Sep/Oct/Nov (SON) season.

Figure 4: Density distributions of projected wind speed changes (m/s) for the selected wind site, four seasons, two policies (L2S and UE), and three SRES scenarios (A2, A1b, and B1)

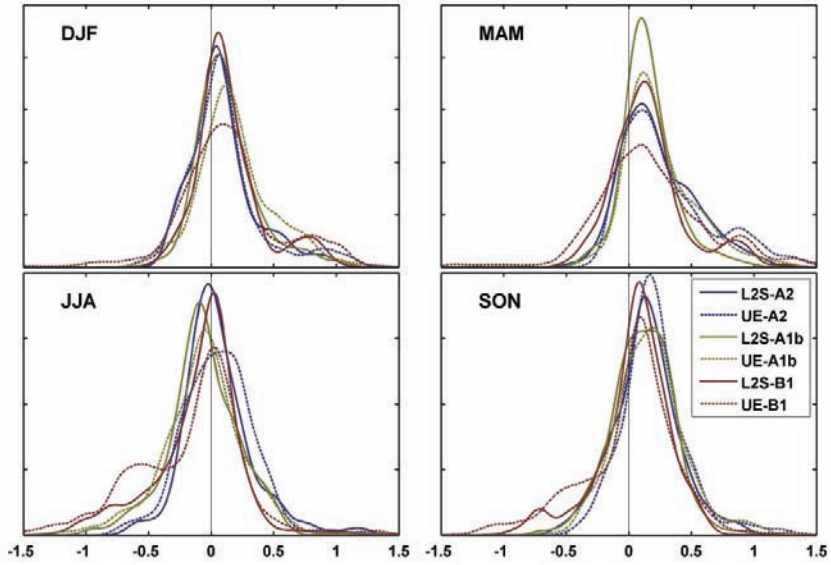

Source: authors' creation.

Figure 5: Density distributions of projected changes in surface solar radiation (W/m^2) for the selected CSP site, four seasons, two policies (L2S and UE), and three SRES scenarios (A2, A1b, and B1)

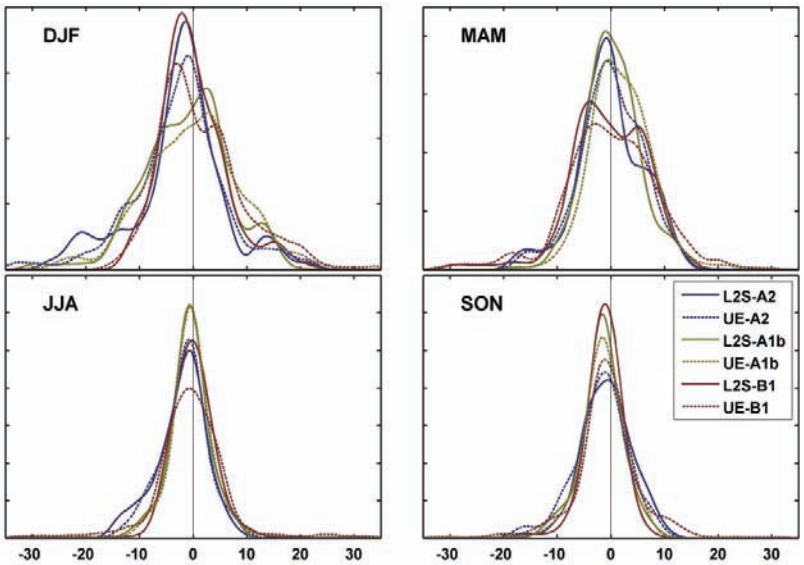

Source: authors' creation.

Figure 6: Geographic and scenario distribution of wind speed changes (m/s) for Jun-Jul-Aug (JJA) using the A1b model results for the statistical model

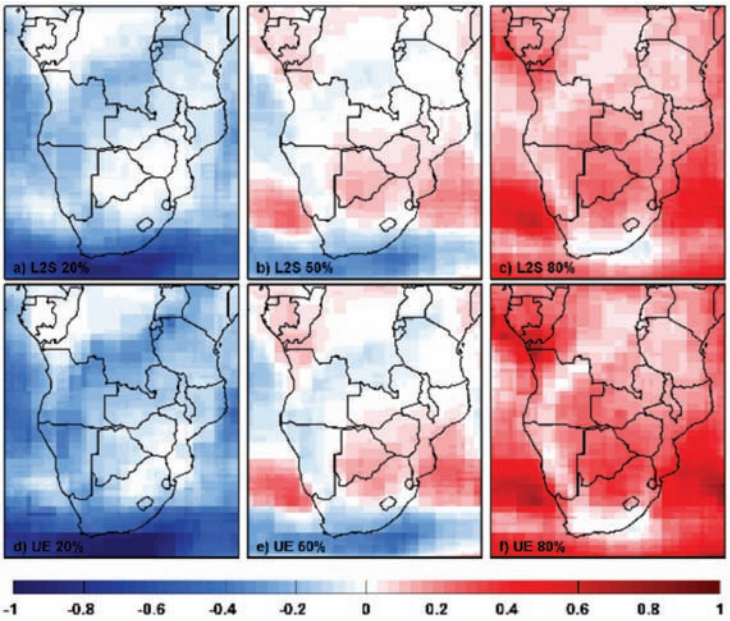

Source: authors' creation.

Note: Subplots a, b, and c show the 20th, 50th, and 80th, percentiles, respectively, for the Level 2 Stabilization (L2S) policy case and d, e, and f show the same percentiles for the Unconstrained Emissions (UE) policy case.

Figure 7: Geographic and scenario distribution of solar radiation (W/m2) changes for Jun–Jul–Aug

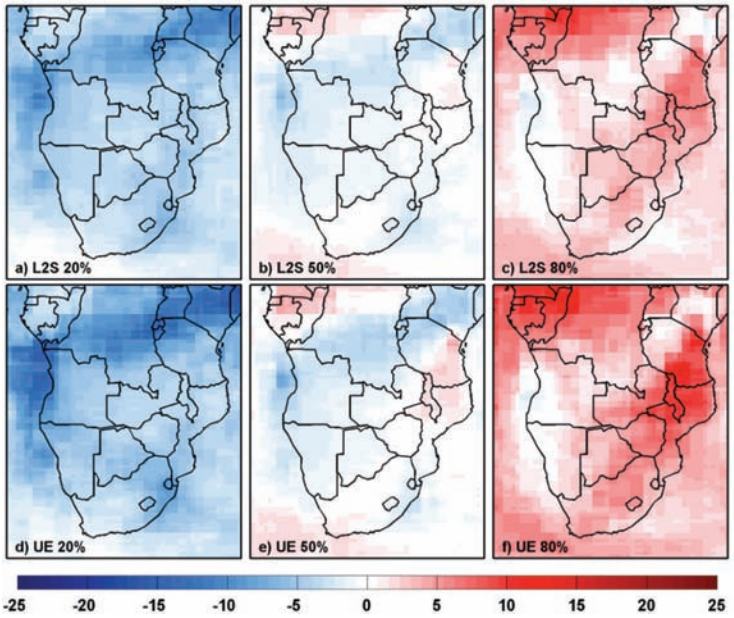

Source: authors' creation.

Note: Subplots a, b, and c show the 20th, 50th, and 80th, percentiles, respectively, for the Level 2 Stabilization policy case and d, e, and f show the same percentiles for the Unconstrained Emissions policy case.